# OVERVIEW AND STATUS OF THE ALICE IR-FEL

D.J. Dunning, N.R. Thompson, J.A. Clarke, ASTeC/CI, STFC Daresbury Laboratory, UK
I. Burrows, D.M.P. Holland, STFC Daresbury Laboratory, Daresbury, UK
S. Leonard, ASTeC/CI/STFC DL & University of Manchester, UK

*Abstract*

The ALICE (Accelerators and Lasers in Combined Experiments) facility (formerly known as ERLP) is being commissioned at Daresbury Laboratory. It is a test facility for novel accelerator and photon science applications. As part of this facility, an oscillator FEL will be commissioned later in 2009. The FEL will be used to test energy recovery with a disrupted beam and to provide output for a select experimental programme. The FEL output will be measured and used to determine the accuracy of FEL modelling techniques. The facility will also be used as a testbed for novel FEL concepts. In this paper, an overview of the FEL design is presented, together with an update of the status of commissioning preparations, including time-dependent modelling using the expected electron beam parameters.

## INTRODUCTION

### *Accelerator and FEL Status*

ALICE (Accelerators and Lasers In Combined Experiments), formerly known as ERLP, is an accelerator R&D facility being commissioned at Daresbury Laboratory. An introduction to the machine and an update of the status of parameters relevant to FEL operation are presented in this section. Further details on the status of ALICE are presented in [1].

The accelerator is an energy recovery superconducting linac designed to operate with a nominal beam energy of 35 MeV. The DC photoelectron gun operates at a nominal voltage of 350 kV with 80 pC bunch charge. The injector can reliably deliver beams with bunch charges >80 pC and with the design temporal structure of 81.25 MHz repetition rate, 100$\mu$s bunch trains, and 1-20 Hz train repetition frequency. Full energy recovery was successfully demonstrated at the end of 2008.

Some of the ALICE design parameters have not yet been achieved. A high voltage insulating ceramic with lower inner diameter than the initial design has been used to increase reliability but this restricts the maximum gun operating voltage to ~250 kV. Provisional beam characterisation has indicated larger emittance values compared to simulations, although improvements are anticipated once a systematic optimisation of the injector setup has been carried out. Due to excessive field emission from the main linac modules the maximum beam energy has been reduced, with the machine being routinely run at 20.8 MeV in commissioning conducted so far, however progress is being made towards achieving higher beam energies with the first operation at >30 MeV achieved mid-August 2009.

Table 1: Nominal ALICE Electron Beam Parameters

| | |
|---|---|
| Electron beam energy | 35 MeV |
| Bunch charge | 80 pC |
| Normalised emittance | 10 mm-mrad |
| Bunch length (rms) | 0.6 ps |
| Energy spread (rms) | 0.1% |

Table 1 summarises the nominal parameters of the ALICE machine.

The accelerator will drive several light sources including an IR-FEL and a Compton Backscattering (CBS) X-ray source. Demonstration of coherently enhanced THz radiation was successfully achieved on ALICE at the beginning of 2009. The FEL undulator and optical cavity will be installed later in 2009.

## FEL DESIGN AND MODELLING

### *FEL Design*

The FEL design was first presented in [2], however an update is warranted. The ALICE IR-FEL is an oscillator-type FEL with a near-concentric optical cavity to minimise the mode size within the undulator and maximise the mode size on the mirrors to reduce thermal loading. The radius of curvature (ROC) of the cavity mirrors has been increased from the original specification of 4.75 m to 4.85 m so that the manufacture specified ROC error tolerances cannot push the cavity into an unstable geometry. For operation with the nominal electron beam parameters, three modes of operation of the FEL are specified. In 'normal mode' the radiation is outcoupled via a 1.5 mm radius hole in the downstream cavity mirror. Further details of the operating modes and full three dimensional, time-dependent modelling of the FEL in each mode were presented in [3].

The FEL undulator is on loan from Jefferson Laboratory where it was previously used for the IR-DEMO FEL project. For implementation in ALICE the undulator has been converted from a fixed-gap to a variable gap device to allow an increased wavelength tuning range, with a full range of ~4-12 $\mu$m achievable through gap tuning (with undulator parameter, $K$=0.7-1.0) and electron beam energy tuning (24-35 MeV). Operating the FEL at the present reduced beam energy of 20.8 MeV will give operation at longer wavelengths (12-16 $\mu$m). The parameters of the ALICE FEL are summarised in Table 2.

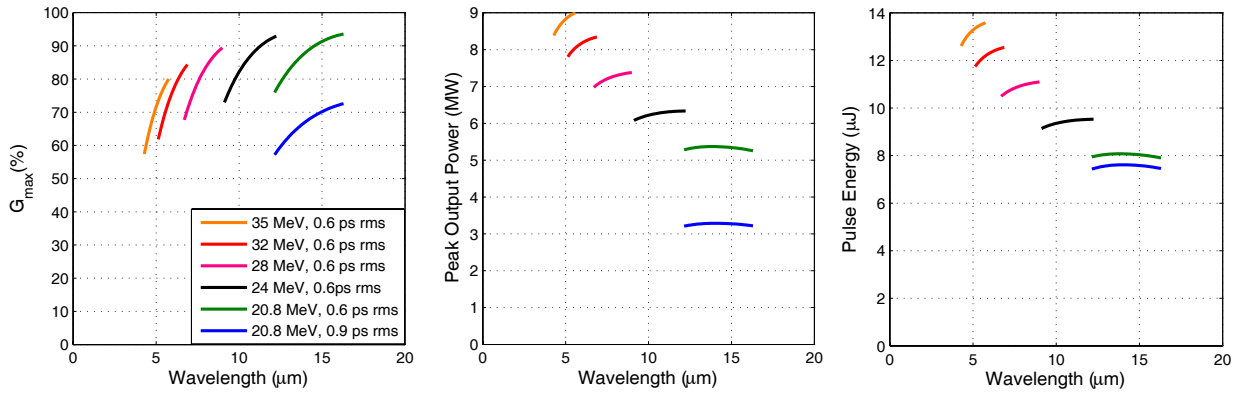


Figure 1: Calculations of single pass gain, peak power output and pulse energy, for different electron beam energies and electron beam rms pulse lengths.

Table 2: ALICE FEL Parameters

| **Parameter** | **Original** | **Present** |
|---|---|---|
| Wiggler period | 0.027 m | 0.027 m |
| Undulator gap | 12 mm | 12-20 mm |
| Number of periods | 40 | 40 |
| Undulator length | 1.08 m | 1.08 m |
| Undulator parameter, K | 1.0 | 0.7-1.0 |
| Optical cavity length | 9.224 m | 9.224 m |
| Cavity mirrors ROC | 4.75 m | 4.85 m |
| Radiation wavelength | 4.4 $\mu$m @ 35 MeV | 4-16 $\mu$m @ 20.8-35 MeV |

## *FEL Output Calculations*

The semi-analytic formulae of [6] have been used to predict the FEL output in the wavelength range 4-16 $\mu$m, with the results presented in Fig. 1. Peak powers in the region of 5-9 MW and pulse energies in the range 8-14 $\mu$J are predicted.

Since full three dimensional, time-dependent modelling of the FEL operating at 4 $\mu$m has already been presented [3], the results presented here are for 16 $\mu$m wavelength operation with a 20.8 MeV beam energy (which can be assumed to be the minimum achievable energy during the first commissioning period). The slippage length $N\lambda_r$ at this wavelength is larger than in the original design: at 16 $\mu$m operation the slippage length is 2.1 ps while the nominal rms electron bunch length is $\sigma_t$=0.6 ps. Time dependent simulations have been done to model the impact of this. Two values of $\sigma_t$ have been used, while conserving the 80pC charge—the nominal length of $\sigma_t$=0.6 ps (giving peak current $I_{pk}$=53.2 A) and $\sigma_t$=0.9 ps (giving $I_{pk}$=34.5 A), with the larger $\sigma_t$ chosen to be the value at which the slippage length is equal to the FWHM bunch length $|\Delta_z|_{FWHM} \simeq 2.35\sigma_z$.

The results of steady-state simulations showing the variation of peak output power against downstream mirror hole radius are given in Fig. 2 (with no hole in the upstream mirror). It is seen by comparing Fig. 1 with Fig. 2 that the peak output powers are close to those predicted by the analytic formulae. It is noted that the case with $I_{pk}$=34.5 A has optimum output at a smaller hole radius (2.5 mm) compared to the $I_{pk}$=53.2 A case (3 mm), since the optimum outcoupling varies with the FEL gain. In both cases the optimum hole radius is larger than that in the nominal FEL design since the transverse size of the radiation on the mirrors scales proportionally to the square root of the radiation wavelength. For first FEL commissioning (at lower than nominal energy) a combination of a 1.5 mm radius hole in the downstream mirror and a 0.75 mm radius hole in the upstream mirror has been chosen (from the nominal mirror sets) to provide output from the downstream hole with a source size compatible with the design of the beam line to the diagnostics room, and to provide local diagnostics at the upstream end. The peak power from the FEL will hence be reduced from the results shown in Fig. 1.

Three dimensional modelling of the FEL has been carried out using Genesis 1.3 [4] in combination with the optics code OPC [5] which models the propagation of the radiation within the optical cavity. The peak power output from the FEL is plotted in Fig. 3 as a function of cavity detuning length, for $\sigma_t$=0.6 ps and $\sigma_t$=0.9 ps. Also shown in Fig. 3 are the evolution of the pulse profiles with cavity round trip, for $\sigma_t$=0.9 ps and cavity detuning lengths of 8 $\mu$m and 40 $\mu$m. It is seen that for a cavity closer to the synchronous length the output power is highest and the pulse length short ($\simeq$0.9 ps FWHM), but takes $\simeq$200 cavity round trips to reach a stable FEL output. For the more detuned cavity length the output reaches stability with fewer round trips, but with lower peak power and longer duration ($\simeq$3.5 ps).

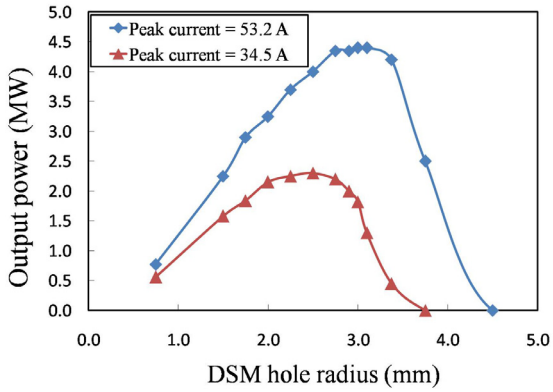


Figure 2: Results of simulations showing the variation of peak output power against downstream mirror hole size, for the two cases of $\sigma_t$=0.6 ps ($I_{pk}$=53.2 A) $\sigma_t$=0.9 ps ($I_{pk}$=34.5 A).

## ALIGNMENT AND COMMISSIONING

The correct alignment of the FEL systems is essential. The magnetic axis of the undulator, the optical axis of the resonator and the electron beam propagation axis must be co-aligned to high precision. With the undulator arrays arranged vertically (such that the $B$-field is horizontal) it has been calculated that the electron beam axis must not deviate from the magnetic axis by more than 200 $\mu$m horizontally and 1 mm vertically. The calculated angular alignment tolerance for the mirrors must satisfy $\theta_m \ll 111\ \mu$rad.

To help achieve these tolerances, the vacuum chamber within the undulator (as supplied on loan from JLAB) comes equipped with three beryllium wedges, each with a 1 mm hole, which can be viewed by CCD cameras, as shown in Fig. 4. These wedges have been pre-aligned to each other within 100 $\mu$m by maximising the transmitted intensity of an externally injected HeNe laser measured on a photodiode. The wedges will then be surveyed on to the magnetic axis of the undulator by use of a laser tracker system. To transversely pre-align the resonator mirrors a HeNe laser alignment module has been developed, as also illustrated in Fig. 4. The HeNe will be injected into the cavity via a 45 degree pop-in mirror and aligned with the holes in the wedges by use of remotely steerable mirrors on the alignment module. The HeNe beam can be brought to a 1 mm focal spot at the wedges with the moveable focussing lens, and the diffraction pattern from a cross-hair target inserted into the HeNe beam provides a useful aid for more precise centering of the HeNe beam on the holes in the wedges. The HeNe beam image as focussed to the wedge within the undulator is also shown on a mock-up paper target in Fig. 4. Once the HeNe beam is correctly aligned with two wedges, the resonator mirror can be adjusted until the reflected HeNe beam is centred on the back face of the central wedge. An identical system is provided for alignment of the other resonator mirror.

With the resonator axis correctly aligned with the holed

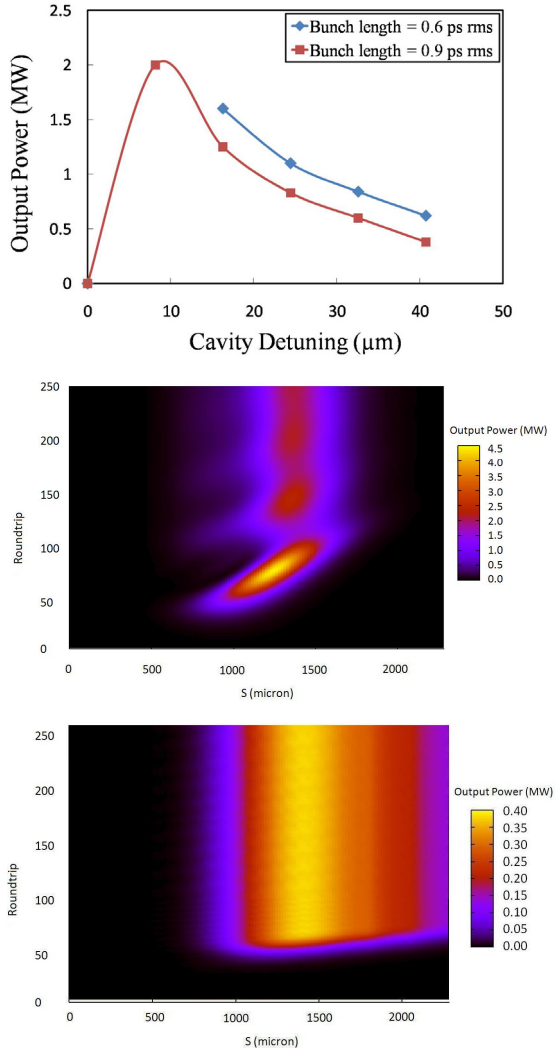


Figure 3: Results of time dependent simulations. The top plot shows peak FEL output power against cavity detuning for $\sigma_t$=0.6 ps and $\sigma_t$=0.9 ps. The middle and bottom plots show pulse profiles against cavity roundtrip for $\sigma_t$=0.9 ps and cavity detuning lengths of 8 $\mu$m (middle) and 40 $\mu$m (bottom).

wedges, and thus with the magnetic axis of the undulator, the electron beam can be steered to the holes in the wedges.

To obtain the correct longtitudinal alignment, the cavity length will be slowly scanned while maximising the intensity of the undulator spontaneous radiation monitored immediately behind the hole in the downstream mirror with an MCT detector. Once this signal saturates and lasing is established, the FEL power will be measured on a power meter immediately behind the hole in the upstream cavity mirror. In this way lasing can be established without the need to correctly transport the IR radiation to the diagnostics room: this will be done in a second phase when the radiation will be fully characterised and transported to the exploitation room for the first experiments.

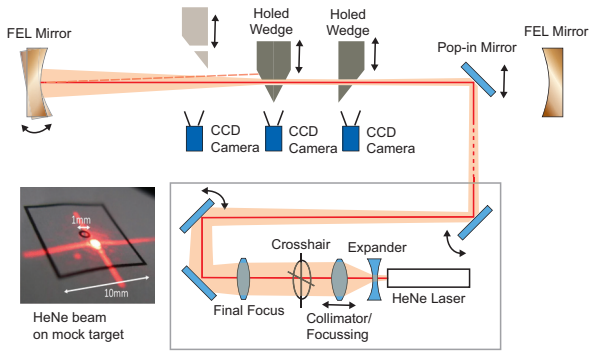


Figure 4: Schematic of the systems to be used for alignment of the FEL optical cavity.

## APPLICATIONS

A select experimental programme is being prepared, focusing on ultrafast probing of molecular dynamics in the strong field regime. Study of excited state molecular photoionisation dynamics, using time-resolved pump-probe techniques, allows the characterisation of energetic and relaxation mechanisms of neutral excited states, improving knowledge of energy flow within matter. In a pump-probe experiment, the pump photon prepares a molecule in an excited intermediate state, and the probe photon ionises the molecule. By monitoring the photoionisation process as a function of the time delay, information is obtained on how the intermediate state evolves with time. Time-resolved photoelectron spectroscopy, where the electron kinetic energies and angular distributions are measured, is well suited to the study of ultrafast molecular dynamics [7].

Single photon (one colour) studies are generally limited by the random alignment of gas phase molecules, reducing the information content of laboratory frame measurements due to rotational smearing. To ameliorate this, it is necessary to define the direction of the molecules in the laboratory frame prior to measurement. A promising approach is to use strong (non-perturbative) non-resonant laser fields to produce molecular axis alignment through interaction with the molecular polarisability. Field-free impulsive alignment, created with laser pulses shorter than the molecular rotational timescales, is an established technique [8]. By focusing the radiation from the IR-FEL, an intensity $> 10^{12}$ W/cm$^2$ can be achieved, sufficient to produce significant alignment in large molecules which have been rotationally cooled following supersonic expansion.

A powerful diagnostic of molecular axis alignment is Coulomb explosion imaging [9]. This requires a synchronised fs laser system to ionise and explode molecules using a high intensity ($>10^{15}$ W/cm$^2$) pulse. A suitable TW laser is available, funded by the North West Development Agency. The distribution of ion fragment recoil velocities, detected with a time and position sensitive imaging spectrometer, characterises the laboratory frame molecular axis distribution. In the time-resolved photoelectron spectroscopy measurements, a single harmonic from an HHG source will be used to ionise the aligned molecules, and an analysis of the photoelectron kinetic energies and angular distributions will reveal the relaxation dynamics.

## CONCLUSION

Strategies for the commissioning of the ALICE IR-FEL are in place and preparations are underway. Modelling of the FEL with the electron beam energy of 20.8 MeV suggests a reduction in peak output power and pulse energy compared to the nominal design but indicate that FEL operation should be achievable. However, recent accelerator commissioning at energy >30 MeV provides the encouraging prospect of obtaining close to the nominal output parameters and wavelength range. The FEL output will be compared to simulations to assess the accuracy of the modelling, then optimised for the user experimental programme. The stability will be assessed and optimised if necessary—techniques such as cavity length stabilisation using an interferometer system have been considered and may be implemented at a later stage.

Proposals are also being developed for novel FEL-related experiments that could be carried out using ALICE to test technologies and techniques of relevance to the UK New Light Source project [10]. For example, some of the advanced FEL concepts proposed for attosecond pulse generation in X-ray FELs could be scaled to the lower beam energies and longer wavelengths (and hence longer output pulses) obtainable with ALICE.

## REFERENCES

[1] S.L. Smith and Y. Saveliev, *The Current Status of the ALICE (Accelerators and Lasers In Combined Experiments) Facility*. These proceedings.

[2] N.R. Thompson et al., *Design for an Infra-Red Oscillator FEL for the 4GLS Energy Recovery Linac Prototype*, Proc. 25th Int. FEL Conf. (Tsukuba, Japan) 2003, p. II-15.

[3] D.J. Dunning et al., *3D Modelling of the ERLP IR-FEL*, Proc. 29th Int. FEL Conf. (Novosibirsk, Russia) 2007, pp. 167-170.

[4] S. Reiche, Nucl. Inst. Meth. Phys. Res. A, **429**, 243, 1999.

[5] J.G. Karssenberg et al., *FEL-Oscillator Simulations with Genesis 1.3*, Proc. 28th Int. FEL Conf. (Berlin, Germany) 2006, pp. 407-410.

[6] F. Ciocci et al., *Insertion Devices for Synchrotron Radiation and Free Electron Laser*, World Scientific, 2000.

[7] A Stolow and J G Underwood, Adv Chem Phys 139 (2008) 497.

[8] H Stapelfeldt and T Seideman, Rev Mod Phys 75 (2003) 543.

[9] P W Dooley, I V Litvinyuk, K F Lee, D M Rayner, M Spanner, D M Villeneuve and P B Corkum, Phys Rev A68 (2003) 023406.

[10] J. Marangos et al., *NLS Science Case & Outline Design Report*, `http://www.newlightsource.org`.